



MINISTRY OF SUPPLY

AERONAUTICAL RESEARCH COUNCIL  
REPORTS AND MEMORANDA

Approximate Calculations of the Laminar  
Boundary Layer with Suction, with Particular  
Reference to the Suction Requirements for  
Boundary-Layer Stability on Aerofoils of  
Different Thickness/Chord Ratios

*By*

M. R. HEAD, D.S.O., D.F.C., M.A., Ph.D.,  
of the Engineering Laboratory, Cambridge University

© Crown copyright 1959

LONDON: HER MAJESTY'S STATIONERY OFFICE

1959

SEVEN SHILLINGS NET

# Approximate Calculations of the Laminar Boundary Layer with Suction, with Particular Reference to the Suction Requirements for Boundary-Layer Stability on Aerofoils of Different Thickness/Chord Ratios

By

M. R. HEAD, D.S.O., D.F.C., M.A., Ph.D.,  
of the Engineering Laboratory, Cambridge University\*

---

*Reports and Memoranda No. 3124*

*September, 1957*

---

1. *General Introduction.*—In an earlier report<sup>1</sup> an account was given of an approximate method for calculating the incompressible laminar boundary layer in two dimensions. Application of the method to the various cases for which exact (or nearly exact) solutions were available gave results which were in all cases in very satisfactory agreement with the accepted solutions. The accuracy of the method (essentially a development of one given earlier by Wieghardt<sup>2</sup>), evidently resulted from satisfying both the momentum and energy integral equations of the boundary layer, together with the first compatibility condition at the surface. The doubly-infinite family of velocity profiles used in the method was obtained by a numerical procedure which gave a very much wider range of physically acceptable profiles than could be achieved by the use of simple analytic expressions (*e.g.*, polynomials).

In the present paper the approximate method just referred to has been applied to the class of problems for which it was specifically devised, namely problems where suction (or blowing) is applied through the surface.

In Part I solutions are given for the following cases:

- (a) Flat plate with uniform suction and sinusoidal variation of external velocity
- (b) Flat plate with intermittent suction
- (c) Suction applied following the normal separation point to maintain a zero skin-friction layer for the flow  $U = 1 - x$
- (d) Flat plate with uniform blowing.

In Part II results are given of comprehensive calculations for a series of aerofoils with related pressure distributions. The distributions of suction required to maintain neutral stability of the boundary layer are given as functions of thickness/chord ratio and Reynolds number. The effect of Mach number is also inferred on certain simplifying assumptions.

---

\* Formerly of the Royal Aircraft Establishment, Farnborough.

## PART I

2. *Flat Plate with Uniform Suction and Sinusoidal Distribution of External Velocity.*—In any practical case the surface over which the boundary layer develops will not be completely flat, and surface waviness is often in practice the cause of premature transition. It is therefore of interest to determine how far the behaviour of the asymptotic layer with suction is modified by the type of pressure distribution to be expected on a wavy surface. This case has already been considered by Spence and Randall in Ref. 3, which will be discussed later.

The particular distribution of external velocity chosen for the present example is

$$U = U_0 \left( 1 + 0.02 \cos 2\pi \frac{x}{c} \right),$$

where  $U$  is the velocity at the edge of the boundary layer,  $U_0$  is the undisturbed stream velocity,  $c$  is a reference length which in this case will be equal to the wavelength, and  $x$  is the distance along the surface.

This corresponds to a variation in  $C_p$  of  $\pm 4$  per cent, which is of the order of the maximum to be expected in practice.

For the flat plate with uniform suction and zero pressure gradient the solution expressed in suitable non-dimensional terms is independent of the particular value of the suction velocity chosen. In particular, the asymptotic momentum thickness  $\theta$  is given by  $\theta v_s/\nu = 0.5$  (or on the basis of the approximate method of Ref. 1 by  $\theta v_s/\nu = 0.512$ ). In the present example, however, a relevant length  $c$  has been introduced and there will be a range of solutions corresponding to different values of  $(v_s/U_0)\sqrt{R_c}$ . It will be noted that this parameter is inversely proportional to  $(\theta_\infty/c)\sqrt{R_c}$  and so expresses in a form independent of Reynolds number the ratio of the asymptotic momentum thickness in zero pressure-gradient conditions to the wavelength of the superimposed pressure distribution. In the present example  $(v_s/U_0)\sqrt{R_c}$  was taken as unity. Thus the results will correspond, for example, to a wavelength of 4 inches, a Reynolds number per foot of  $2 \times 10^6$  and a suction velocity ratio  $v_s/U_0 = 0.0012$ . It may be expected that the asymptotic value of  $\theta$  will vary regularly about a mean value, which is in the region of the asymptotic value for zero pressure-gradient conditions.

The calculation was started by assuming that at  $x = 0$  the values of  $l$ ,  $m$  and  $(\theta/c)\sqrt{R_c}$  were those appropriate to the asymptotic solution in zero pressure-gradient conditions. The calculation was then carried out over several wavelengths but it became obvious that to obtain a close approximation to the final values in this way would require considerable time. Trial of different starting values was therefore resorted to and after several attempts values were obtained by interpolation which gave precisely the same value for  $(\theta/c)\sqrt{R_c}$  at  $x/c = 1$  as at  $x/c = 0$  and values of  $l$  and  $m$  which differed only very slightly. This final calculation was accepted as giving a close approximation to asymptotic conditions.

The results of the calculations are shown in Figs. 1, 2 and 3. It will be seen from Fig. 1 that  $H$ ,  $(\theta/c)^2 R_c$  and the dimensionless skin friction  $(c/U) (\partial u/\partial y)_0 R_c^{-1/2}$  all vary approximately sinusoidally, but that the maximum of  $H$  and the minimum of  $(c/U) (\partial u/\partial y)_0 R_c^{-1/2}$  occur appreciably before the position of maximum pressure. Rather surprisingly the maximum value of  $(\theta/c)^2 R_c$  is also displaced in the same direction. It will be seen that the mean value of this quantity is somewhat greater than the asymptotic value for zero pressure gradient. The  $l$ ,  $m$  curve traced out in the calculation takes roughly the form of an ellipse with the asymptotic values for zero pressure gradient near the centre. This naturally results from the fact that  $l$  and  $m$  vary approximately sinusoidally but somewhat out of phase with each other, about the zero pressure gradient values as an approximate mean.

From Figs. 2 and 56 of Ref. 1,  $R_{\theta \text{ crit}}$  is found to vary from about 19,500 to 20,500. In view of the large margin between either of these and the largest values of  $R_\theta$  encountered in practice, this variation is scarcely significant.

Turning now to Ref. 3, two criticisms may be offered of the results presented there. First, it appears unrealistic to assume that for the maintenance of laminar flow it is necessary on a wavy surface to increase the overall suction so that no profile should be formally unstable. In fact, if the suction is maintained unaltered at the zero pressure-gradient value, then the added stability introduced by the favourable pressure gradients in the case of the wavy surface is likely to offset very largely the reduced stability due to the adverse pressure gradients, so that the net destabilising effect is likely to be relatively small; moreover, the variations in pressure considered in Ref. 3 are much more extreme than are likely to be encountered in practice. A more serious criticism is that, in considering the stability of the profiles, the form parameter  $H$  was taken as an index of stability. In the case of the profiles normally obtained, which constitute very closely a one-parameter family, this assumption is reasonably well justified<sup>4</sup>. However, in the case of the extreme profiles considered by Spence and Randall, Fig. 56 of Ref. 1 suggests that this assumption may lead to very considerable error, since lines of constant  $R_{\theta \text{ crit}}$ , when plotted as functions of  $l$  and  $m$  are far from coincident with lines of constant  $H$ .

3. *Flat Plate with Intermittent Suction.*—This is a somewhat similar problem to that discussed in the previous Section, but instead of a regularly varying external pressure distribution the boundary layer is now subjected to a regularly varying distribution of suction. A sinusoidal distribution of suction velocity might have been chosen but this is a problem of little practical interest; a more important case is that of substantially uniform suction interrupted at regular intervals by spanwise strips through which suction is not applied. Interest in this problem arises from the practical necessity for supporting any porous or perforated surface used for boundary-layer control, so that the distribution of suction is not in fact continuous.

The present calculation was undertaken in connection with wind-tunnel tests of suction applied through a uniformly perforated sheet supported on regularly spaced spanwise strips. The relevant dimensions of the experimental arrangement are shown in Fig. 4. For convenience the reference length  $c$  was taken as one inch, the tunnel speed chosen giving a Reynolds number based on  $c$  of  $3.2 \times 10^4$ . A suction velocity ratio 0.01 in the regions where suction was applied then gave  $(v_s/U_0)\sqrt{R_c}$  the value 1.8. Using this value of  $v_s^*$  the problem was then solved substantially in the same way as that of the previous Section. Initial values corresponding to asymptotic conditions with uniformly distributed suction were first taken and the development of the boundary layer over successive strips calculated. Again it was found that asymptotic conditions were approached only slowly, so that it was necessary to resort to trial and interpolation to find starting values which gave the same values of  $(\theta/c)\sqrt{R_c}$  and of  $l$  and  $m$  at the beginning and end of the interval. The momentum and energy thicknesses were maintained constant at the discontinuities in suction velocity, the values of  $l$  and  $m$  following any discontinuity therefore being chosen so that  $H_s$  remained unaltered while the new boundary condition at the surface was satisfied.

The results of the calculations are shown in Figs. 5 and 6. Fig. 5 shows the variation of  $(\theta/c)\sqrt{R_c}$  and the dimensionless skin friction parameter  $(c/U)(\partial u/\partial y)_0 R_c^{-1/2}$  over rather more than one interval. Shown also on the figure for comparison are the asymptotic values for the same total suction quantity uniformly distributed. The closed  $l, m$  curve followed in the calculations is shown in Fig. 6 along with velocity profiles for points just off and just on the suction strips. It will be noted that the results presented are applicable (in the absence of a pressure gradient and sufficiently far downstream), to any configuration where the width of the porous strips is four times that of the impervious strips and where  $(v_s/U_0)\sqrt{R_c}$  has the value 1.8, the reference length  $c$  being chosen as twice the width of the porous strips.

From Fig. 6 it will be seen that with suction intermittently applied, the mean momentum thickness is appreciably greater than with uniformly distributed suction. However, the mean skin friction must be the same, since in each case the net boundary-layer growth due to skin friction must just balance the net decrease due to suction, which is the same in the two cases. The fact that the means do check closely is some measure of the accuracy of the calculations. From the velocity profiles shown in Fig. 6 it will be seen that over the width of the impervious

strip the boundary layer increases very considerably in thickness and takes on a form resembling the Blasius. For the value of  $R_c$  given earlier ( $3.2 \times 10^4$ ) the width of the strip is found to be approximately five boundary-layer thicknesses, so that the changes take place exceedingly rapidly. The discontinuities in skin friction and the relatively smaller discontinuities in profile shape occurring at the junctions of the porous and impervious strips represent minor shortcomings of the approximate method used here.

4. *Preservation of a Zero Skin-Friction Layer by Suction.*—Calculation of the Howarth flow  $\bar{U} = 1 - \bar{x}$  (or the equivalent  $U = b_0 - b_1x$ ) has been given in Section 3.2 of Ref. 1. There it was seen that the layer separated (*i.e.*, the skin friction dropped to zero) at  $\bar{x} = 0.12$ . The present calculation was carried out to find the distribution of suction applied at and beyond that point which would just maintain the layer in the unseparated condition with the skin friction zero. Unlike, for example, methods of the Pohlausen type, the present method would be expected to show a change in profile shape as the zero skin-friction layer develops under the influence of suction. Thwaites has considered the case and present results are compared below with those given in Ref. 5.

The calculation method for the present example was developed as follows:

For zero skin-friction, equations (1), (2) and (3) of Ref. 1 become respectively

$$H_e' = \frac{1}{\bar{U}t^*} \left[ 2D^* - H_e \left\{ -A(H-1) - \lambda \right\} \right] \dots \dots \dots (1)$$

$$t^{*'} = \frac{2}{\bar{U}} \left[ -\{A(H+2) - \lambda\} \right] \dots \dots \dots (2)$$

$$m = -A.$$

$A$  may therefore be replaced by  $-m$ , and for  $l = 0$ ,  $D^*$ ,  $H$ , and  $H_e$  are functions only of  $m$ .

If, for  $l = 0$ , we let  $A(m) = m(H+2)$ ,  $B(m) = 2D^* - H_e m(H-1)$ ,  $C(m) = H_e - 1$  and  $D(m) = dH_e/dm$ , then (1) and (2) may be written

$$D \frac{dm}{dx} = \frac{1}{\bar{U}t^*} [B + C\lambda] \dots \dots \dots (3)$$

$$\frac{dt^*}{d\bar{x}} = \frac{2}{\bar{U}} [A - \lambda]. \dots \dots \dots (4)$$

Now for the present case  $\bar{U} = 1 - \bar{x}$ .

Hence  $m = -A = -t^*\bar{U}' = t^*$ ,  $\dots \dots \dots$  (5)

so that (3) and (4) may be written

$$\frac{dm}{d\bar{x}} = \frac{1}{Dm(1-\bar{x})} [B + C\lambda]$$

$$\frac{dm}{d\bar{x}} = \frac{2}{1-\bar{x}} [A - \lambda].$$

Equating the two expressions for  $dm/d\bar{x}$  and simplifying, we have

$$\lambda = \frac{2DmA - B}{2Dm + C}.$$

Or, if we write  $E(m) = 2Dm$ , then

$$\lambda = \frac{EA - B}{E + C} \dots \dots \dots (6)$$

Thus, for any value of  $m$ ,  $\lambda$  is uniquely determined by the necessity for satisfying both the energy and momentum equations and the condition that  $l = 0$ . Or we may say that equation (6) follows

from the fact that  $\lambda$  must be chosen at each stage so that the increment in  $m$  which follows from the momentum equation is compatible with the change in  $H_e$  obtained from the energy equation,  $H_e$  being uniquely determined by  $m$  for  $l = 0$ .

$A$ ,  $B$ ,  $C$  and  $E$  are quantities which may be readily obtained from the charts, so that  $\lambda$  can be plotted as a function of  $m$  over the range available. From this curve and the momentum equation, which we may now write  $m' = (2/\bar{U})(A - \lambda)$ , the solution to the present problem may readily be obtained, using as starting values the separation profile obtained in Section 3.2 of Ref. 1.

The solution was carried only as far as  $\bar{x} = 0.22$ , in order to keep within the range of the present charts; it would have been quite reasonable to pursue the calculation further by extrapolating the curves of  $\lambda$  and  $\bar{U}m'/2$  plotted against  $m$  (see Fig. 7). However, the main features of the solution seem clear; as the zero skin-friction boundary layer develops, the value of  $m$  (i.e., the curvature of the profile at the surface), steadily increases, while  $H$  decreases. This may be seen from Fig. 8 which shows several boundary-layer velocity profiles for different values of  $x$ . Fig. 9 shows the growth of momentum thickness and Fig. 10 compares the distribution of suction velocity with that given by Thwaites<sup>5</sup>. It will be seen that the present result differs appreciably from that obtained by Thwaites; in particular, the present method shows that appreciable suction velocities are required right from the point where the skin friction reaches zero. This is a very reasonable result, since the whole course of development of the boundary layer must be discontinuously changed at this point.

5. *Flat Plate with Uniform Blowing*.—Though probably of small practical importance, this problem is of some interest because of its complementary relationship to the case of uniform suction. By the method of Ref. 1 it may be treated in exactly the same way, the relevant equations being most conveniently expressed, as for suction, in the following way:

$$\lambda^{2'} = 2(l - \lambda)$$

$$H_e' = \frac{1}{\lambda^2} \{2D^* - H_e(l - \lambda) - \lambda\},$$

where the primes here denote differentiation with respect to  $\xi \equiv (v_s/U)^2 R_x$ , and  $m = -l\lambda$ . For blowing,  $v_s$  will be negative, so that the sign of  $\lambda$  will now be changed (but not that of  $\xi$  or  $\lambda^2$ ). The calculation is found to proceed satisfactorily up to a value of  $\xi$  of approximately 0.35 or 0.4, the main features of the flow following those which might intuitively be expected; the skin friction, and values of  $l$ , steadily diminish along the plate and the rate of growth of  $\theta$  with  $x$  (or of  $\lambda$  with  $\xi$ ) tends to the constant value given by  $d\theta/dx = -v_s/U$  (or  $d\lambda/d\xi = -1$ ). The value of  $m$  is found to reach a maximum of approximately 0.034 at  $\xi = 0.15$  and thereafter decreases fairly rapidly.

As the solution proceeds and the values of  $l$  and  $m$  diminish, the present method becomes increasingly difficult to apply, partly because of the reduced accuracy associated with using graphical methods in the small neighbourhood of  $l = 0$ ,  $m = 0$ , and partly because of the increased sensitivity of the solution to small errors in the preparation of the charts in this region, which ultimately makes it impossible to satisfy simultaneously the three governing equations. The detailed solution is therefore given only as far as  $\xi = 0.36$ , at which point  $l$  has fallen to 0.037 and  $m$  to 0.021. It is not unreasonable to suppose that both  $l$  and  $m$  should continue to fall with increasing  $\xi$  and should ultimately reduce to zero; if this is the case, however, it should be noted that the orders of zeroes of  $m$  and  $l$  must be different, since as  $\xi \rightarrow \infty$ ,  $\lambda$  (and hence  $m/l$ )  $\rightarrow \infty$ . Alternatively  $m$  may tend to a small but finite value as  $l$  tends to zero, though there is no reason to expect that this should be so. In any case it appears that the limiting velocity profile will correspond very closely to that for  $l = 0$ ,  $m = 0$ .

The results of the calculation are shown in Figs. 11, 12 and 13. Fig. 11 gives boundary-layer velocity profiles for various values of  $\xi$ , Fig. 12 compares the boundary-layer development with uniform blowing with that for uniform suction, while Fig. 13 shows the  $l$ ,  $m$  curves for the two cases. This last Figure clearly shows the complementary character of the two solutions.

## PART II

6. *Suction Applied to Maintain Boundary-Layer Stability on Aerofoils of Different Thickness/Chord Ratios.*—6.1. *Introduction.*—Experiments have shown that distributed suction is an effective means of achieving extensive laminar flow in effectively two-dimensional conditions. Stability theory, developed mainly in Germany by Schlichting and others, provides the basis for theoretical estimates of the suction quantities required to prevent transition; according to this theory, so long as the boundary-layer Reynolds number is maintained at every point below the critical value associated with the velocity profile at that point, then transition due to the amplification of small disturbances cannot occur. Stability theory has received substantial experimental verification and estimates of the suction quantities required to maintain stability of the laminar boundary layer have in general been found to agree satisfactorily with the suction requirements for laminar flow. Calculations performed in the past have been confined to particular pressure distributions, and the object of the present investigation has been to obtain results which are sufficiently comprehensive to allow the variation of minimum suction quantities with thickness/chord ratio, Reynolds number, Mach number and design lift coefficient to be inferred.

In Ref. 1 a chart is provided showing how the critical boundary-layer Reynolds number is related to the different profiles of the given doubly-infinite series. It is therefore possible, after calculating the boundary-layer development for any particular distribution of suction, to determine whether, at any point, the actual boundary-layer Reynolds number exceeds the critical value at that point; if not, it may be concluded that the suction distribution chosen will be effective in preventing transition.

A further development is made possible by superimposing the curves of  $R_{\theta \text{ crit}}$  (Fig. 56 of Ref. 1) on the chart of  $H_e$  (Fig. 1 of the same report). This has been done in Fig. 14. The calculation can then be carried out, step by step, so that at each point the suction is given the value which will make  $R_\theta$  equal to  $R_{\theta \text{ crit}}$ . With this distribution of suction, the boundary layer will be in a condition of uniform neutral stability and the overall suction requirement may be expected to approximate closely the minimum compatible with laminar flow. In the present calculations, distributions of suction velocity have been found in this way for each of four pressure distributions at three Reynolds numbers covering the range of practical interest. Details of the procedure and the results obtained are given in the following Sections. The notation is that given at the end of the report.

6.2. *Procedure.*—A family of related pressure distributions was obtained by choosing the theoretical distribution for aerofoil NACA 65,021 at zero incidence, and varying the scale of  $w/U_0$  (where  $w = U - U_0$ ) to give distributions corresponding to aerofoils of different thickness/chord ratio. The basic velocity distribution and those derived from it are shown in Figs. 15 and 16. The nominal thickness/chord ratios quoted in Fig. 15 and in the four subsequent Figures are based on the assumption that these ratios are proportional to the scale of  $w/U_0$ . This is approximately true, but in fact the nominal thickness/chord ratios are used simply as a means of reference to the particular distributions of velocity shown in the Figure.

The following procedure was used to calculate the development of the boundary layer for a given chord Reynolds number and distribution of external velocity:

Calculations were started at  $2\frac{1}{2}$  per cent chord, at which point the values of  $l$  and  $m$  were assumed in all cases to be 0.350 and  $-0.073$  respectively. This assumption is justified by the highly favourable pressure gradient existing over the first few per cent of the chord; in these conditions, arbitrarily chosen values of  $l$  and  $m$  will rapidly approach the correct values as the calculation proceeds through the initial steps. Up to a certain chordwise position (which depended upon the pressure distribution and the chord Reynolds number), the values of  $R_\theta$  were obtained which were less than the values of  $R_{\theta \text{ crit}}$  for the corresponding values of  $l$  and  $m$ . In this region it was obviously unnecessary to apply suction. At some point, however, the values

of  $R_\theta$  and  $R_{\theta \text{ crit}}$  coincided, and beyond this point it was necessary to apply suction in order to maintain neutral stability of the boundary layer. Here the calculation was carried out in the following way: The momentum equation was used in the normal fashion to find the value of  $(\theta/c)\sqrt{R_c}$  at the end of a step. From the known values of  $R_c$  and  $U/U_0$  the value of  $R_\theta$  then followed, and for neutral boundary-layer stability this was evidently also the value of  $R_{\theta \text{ crit}}$ . The value of  $H_e$  was known from the energy equation, and the point of intersection of the curves of  $H_e$  and  $R_{\theta \text{ crit}}$  (see Fig. 13) gave the appropriate values of  $l$  and  $m$ . The value of  $\lambda$  followed from the first compatibility condition at the surface, thus enabling the calculation to be carried through a further step. From the values of  $\lambda$  and  $R_\theta$  at each point the corresponding value of  $v_s/U$  followed, and in this way the complete chordwise distribution of suction for neutral stability of the boundary layer was determined.

Fig. 17 shows the calculated distributions of suction velocity for a chord Reynolds number of  $20 \times 10^6$ , and Fig. 18 compares the distributions of suction velocity for two different thickness/chord ratios at chord Reynolds numbers of 4, 20 and 100 millions. Fig. 19 shows calculated velocity profiles at various chordwise positions.

6.3. *Effect of a Small Increase in Suction Velocity.*—The calculations for a particular velocity distribution and chord Reynolds number were repeated with the suction velocities increased by 10 per cent. at all points. The stability of the boundary layer was increased markedly in the region of adverse pressure gradient, as may be seen from Fig. 20, the value of the ratio  $R_{\theta \text{ crit}}/R_\theta$  at the trailing edge being increased by a factor of approximately 3.5. A similar increase of suction would have had an even more considerable effect in the case of velocity distributions corresponding to aerofoils of greater thickness/chord ratio, and it therefore appears that it would require very substantial errors in the values of  $R_{\theta \text{ crit}}$  given in the charts to affect appreciably the calculated suction quantities to maintain boundary-layer stability. It may also be concluded that small increases in suction have a disproportionate stabilising effect on the boundary layer.

6.4. *Variation of Minimum-Suction Quantities with Thickness/Chord Ratio and Reynolds Number.*—Data from Ref. 6 show that neither the thickness/chord ratios nor the velocity distributions for the NACA 65 series of aerofoils conform precisely to the related distributions considered, and although the discrepancies are fairly small it was considered worthwhile to take account of them, at least to a first approximation. To do this the calculated values of  $C_\theta$  were plotted for each of the three Reynolds numbers as functions of  $C_{p \text{ min}}$ , the minimum pressure coefficients on the aerofoil surface. The values of  $C_\theta$  corresponding to any symmetrical aerofoil of the NACA 65 series were then obtained using the value of  $C_{p \text{ min}}$  for that particular aerofoil. The curves of  $C_\theta$  plotted against thickness/chord ratio and Reynolds number are shown in Fig. 21. It will be seen that at normal-flight Reynolds numbers the suction requirements for even a very thick aerofoil are still quite small.

6.5. *Variations of Minimum-Suction Quantities with Mach Number.*—To obtain the curves given in Fig. 22 it was assumed that Mach number was important only in so far as it affected the pressure distribution over the surface. Thus it was assumed that compressibility had no direct effect either on the distribution of velocity within the boundary layer or on the stability of the boundary layer for a given distribution of velocity within it. Neither of these assumptions is strictly correct but it is believed that up to local Mach numbers of unity the errors introduced will be small.

For any particular Mach number the pressure distribution around a given aerofoil will be similar to that about an equivalent aerofoil of greater thickness/chord ratio in incompressible flow. The thickness/chord ratio of the equivalent aerofoil may be found from the Prandtl-Glauert or Kármán-Tsien rules, the latter being used in the present calculations. The suction quantity required to maintain neutral stability of the boundary layer on the equivalent thicker aerofoil in incompressible flow may then be taken as the appropriate value for any particular high-Mach-number case.

6.6. *Variation of Minimum-Suction Quantity with Design  $C_L$ .*—If we take a constant-loading camber-line, then we may expect that to a close approximation the suction requirement over the upper surface will be increased in the ratio  $\sqrt{\{(U_0 + w_c)/U_0\}}$ , while that for the lower surface will be decreased in the ratio  $\sqrt{\{(U_0 - w_c)/U_0\}}$  (here  $w_c$  is the additional velocity over the upper surface due to camber). To a first approximation the total suction requirement will therefore remain unaltered. For other types of camber-line there may be some increase in suction requirement but it seems likely that this will be small.

6.7. *Calculation for Zero Suction.*—For a particular distribution of external velocity the development of the laminar boundary layer without suction was calculated up to the separation point, which occurred at approximately 51·5 per cent chord. The results of the calculation are shown in Fig. 23 compared with the corresponding results for the suction case. It may be of interest to record that the value of  $l$  at the pressure minimum was 0·252 (*cf.* the Blasius value 0·221) and the value of  $m$  at separation 0·163 (*cf.* the value 0·0682 for Hartree's similar profiles, and 0·085 assumed by Thwaites). It is believed that these results are reasonably accurate and reflect the effect of the rapid change in pressure gradient in the region of the pressure minimum.

7. *Concluding Remarks.*—The examples treated in this report show the versatility of the calculation method given in Ref. 1. No case has so far been encountered where the method breaks down for any fundamental reason, though occasionally (for example, in the case of concentrated strip suction not treated here), the range of the charts is insufficient to allow a complete solution to be obtained; in the case of the flat plate with uniform blowing (Section 5), it will be remembered that the accuracy of the charts was evidently insufficient (in the region close to  $l = 0, m = 0$ ), to allow the problem to be formally completed. In general, however, the method has been found very satisfactory for a class of problems which would at best be only inadequately treated by the use of the momentum equation alone.

8. *Acknowledgements.*—The calculations described in Section 6 were carried out while the author was at the Royal Aircraft Establishment, and acknowledgements are due to the Director of the Establishment for permission to publish the results, and to Miss Jean Wilson for carrying out the computing work. The author is also grateful to Mr. D. Johnson and Dr. R. A. Dutton for their assistance.

## NOTATION

$U_0$	Undisturbed stream velocity
$U$	Local velocity outside boundary layer
$w = U - U_0$	
$w_c$	Velocity increment due to camber
$u$	Tangential velocity at any point in the boundary layer
$v_s$	Suction velocity
$Q$	Suction quantity per sec per unit span
$= \oint v_s ds$	
$p_0$	Undisturbed stream static pressure
$p$	Local static pressure
$s$	Distance along the surface
$x$	Distance along the chord, taken for the calculations as equal to the distance along the surface
$y$	Distance normal to the surface
$c$	Chord or chosen reference length
$\theta$	Momentum thickness
$= \int_0^\infty \frac{u}{U} \left(1 - \frac{u}{U}\right) dy$	
$\theta_\infty$	Asymptotic momentum thickness
$\delta^*$	Displacement thickness
$= \int_0^\infty \left(1 - \frac{u}{U}\right) dy$	
$\varepsilon$	Energy thickness
$= \int_0^\infty \frac{u}{U} \left\{1 - \left(\frac{u}{U}\right)^2\right\} dy$	
$\nu$	Kinematic viscosity
$\rho$	Density

### Dimensionless

$\bar{u} = U/U_0$	
$\bar{x} = x/c$	
$R_c = U_0 c / \nu$	Reynolds number based on $c = U_0 c / \nu$
$R_x = U_0 x / \nu$	Reynolds number based on $x = U_0 x / \nu$
$R_\theta = U_0 \theta / \nu$	Reynolds number based on $\theta = U_0 \theta / \nu$
$R_{\theta \text{ crit}}$	Critical value of $R_\theta$

NOTATION—*continued*

$C_p$	Pressure coefficient
	$= \frac{p - p_0}{\frac{1}{2}\rho U_0^2}$
$C_0$	Suction quantity coefficient
	$= \frac{Q}{U_0 c}$
$H$	$= \delta^*/\theta$
$H_e$	$= \varepsilon/\theta$
$D^*$	Dissipation integral
	$= \int_0^\infty \left(\frac{\theta}{U}\right)^2 \left(\frac{\partial u}{\partial y}\right)^2 d\left(\frac{y}{\theta}\right)$
$A$	Pressure-gradient parameter
	$= \frac{\theta^2 dU}{\nu dx}$
$\lambda$	Suction parameter
	$= \frac{\theta v_s}{\nu}$
$\xi$	$= \left(\frac{v_s}{U_0}\right)^2 R_x$
$v_s^*$	$= \frac{v_s}{U_0} \sqrt{R_c}$
$t^*$	$= \left(\frac{\theta}{c}\right)^2 R_c$
$l$	$= \frac{\theta}{U} \left(\frac{\partial u}{\partial y}\right)_0$
$m$	$= \frac{\theta^2}{U} \left(\frac{\partial^2 u}{\partial y^2}\right)_0$

Subscript  $_0$  refers to conditions at the surface.

$A, B, C, D$  and  $E$  are functions of  $m$  (for  $l = 0$ ) defined in Section 4.

Except where otherwise specified, primes denote differentiation with respect to  $\bar{x}$ .

## REFERENCES

- | <i>No.</i> | <i>Author</i>                       | <i>Title, etc.</i>  |
|------------|-------------------------------------|---|
| 1          | M. R. Head .. .. .                  | An approximate method of calculating the laminar boundary layer boundary layer in two-dimensional incompressible flow. R. & M. 3123. March, 1957.           |
| 2          | K. Wieghardt .. .. .                | On an energy equation for the calculation of laminar boundary layers. MAP-VG 109-89T. A.R.C. 9825. June, 1946.  |
| 3          | D. A. Spence and D. G. Randall ..   | The influence of surface waves on the stability of a laminar boundary layer with uniform suction. C.P. 161. March, 1953.                                    |
| 4          | P. Chiarulli and J. C. Freeman ..   | Stability of the boundary layer. Monograph VI. U.S.A. Air Material Command Technical Report F-TR-1197-IA. TIB No. P.36611. 1948.                            |
| 5          | B. Thwaites .. .. .                 | The development of laminar boundary layers under conditions of continuous suction. Part II.—Approximate methods of solution. A.R.C. 12,699. November, 1949. |
| 6          | I. H. Abbott and A. E. von Doenhoff | <i>Theory of Wing Sections.</i> McGraw-Hill. 1949.  |

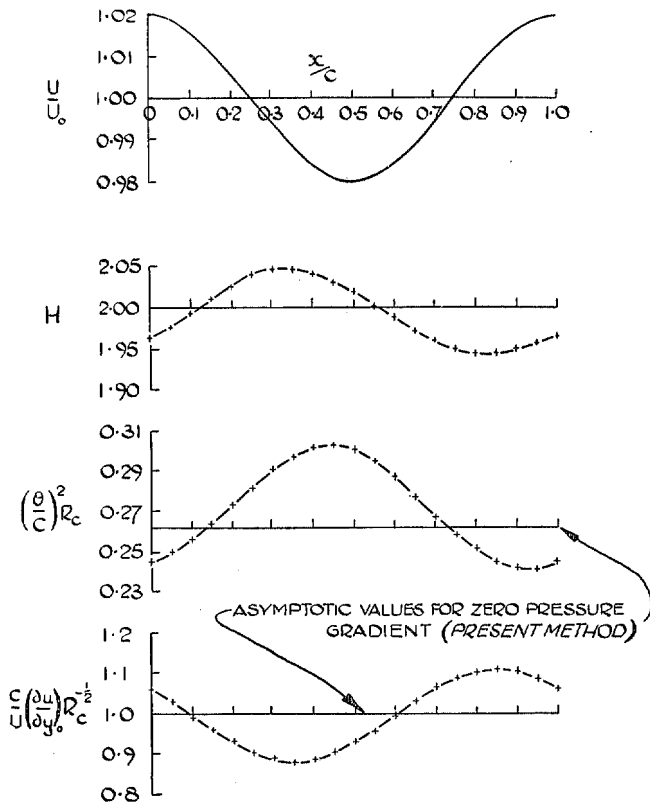


FIG. 1. Asymptotic solution for flat plate with uniform suction and sinusoidal velocity distribution given by  $U = U_0\{1 + 0.02 \cos 2\pi (X/L)\}$ , for  $v_s/U_0\sqrt{R_c} = 1.0$ .

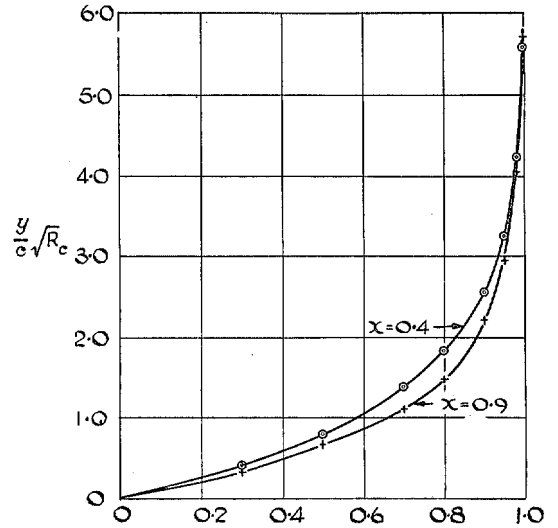


FIG. 3. Velocity profiles for flat plate with uniform suction and sinusoidal pressure distribution.

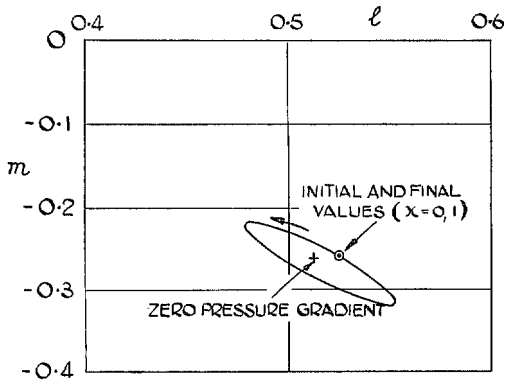


FIG. 2.  $l, m$  values for flat plate with uniform suction and sinusoidal pressure distribution.

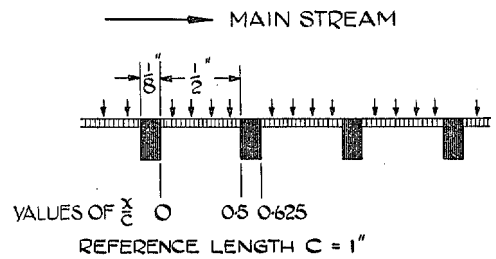


FIG. 4. Suction configuration.

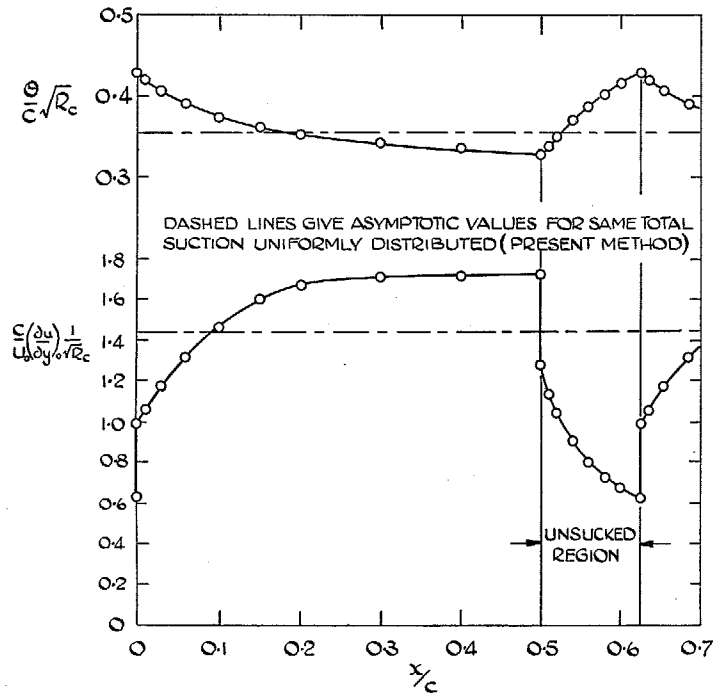


FIG. 5. Asymptotic distributions of momentum thickness and skin friction for flat plate with intermittent suction.

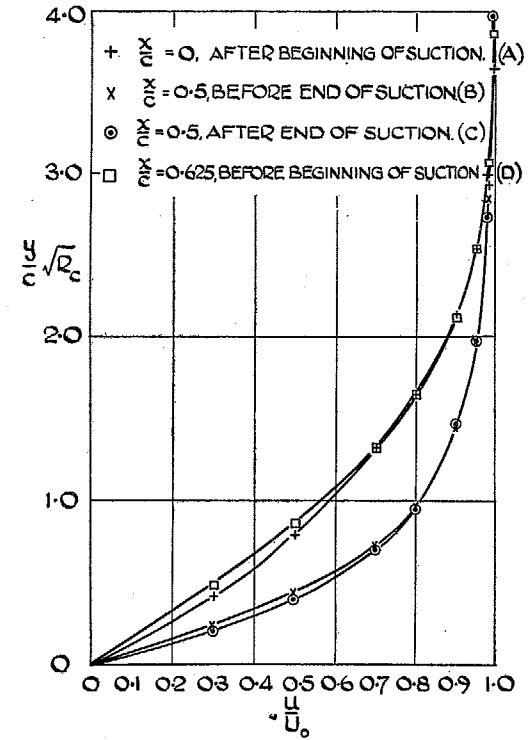
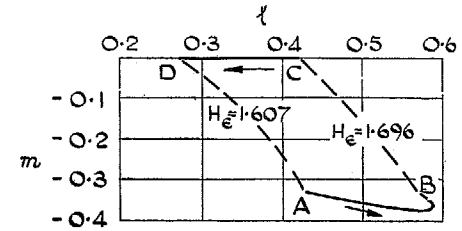


FIG. 6.  $l, m$  curves and velocity profiles for flat plate with intermittent suction.

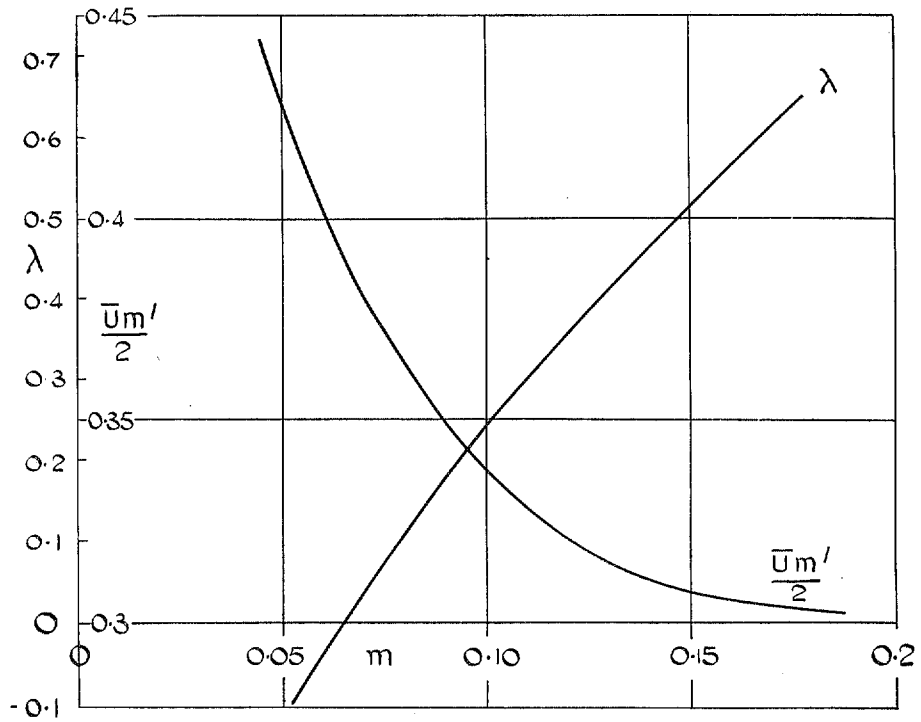


FIG. 7.  $\lambda$  and  $\bar{U}m'/2$  plotted as functions of  $m$ .

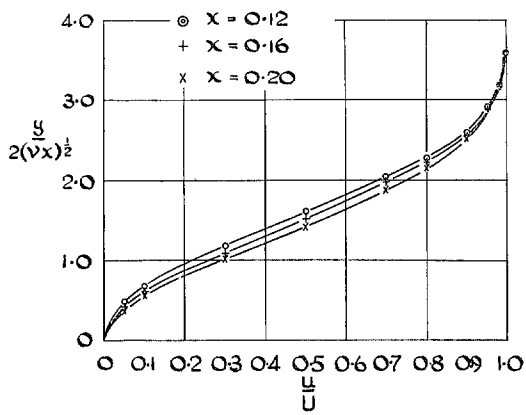


FIG. 8. Velocity profiles for zero skin-friction layer.

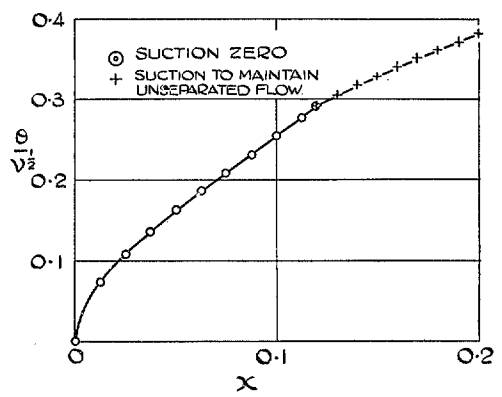


FIG. 9. Growth of momentum thickness.

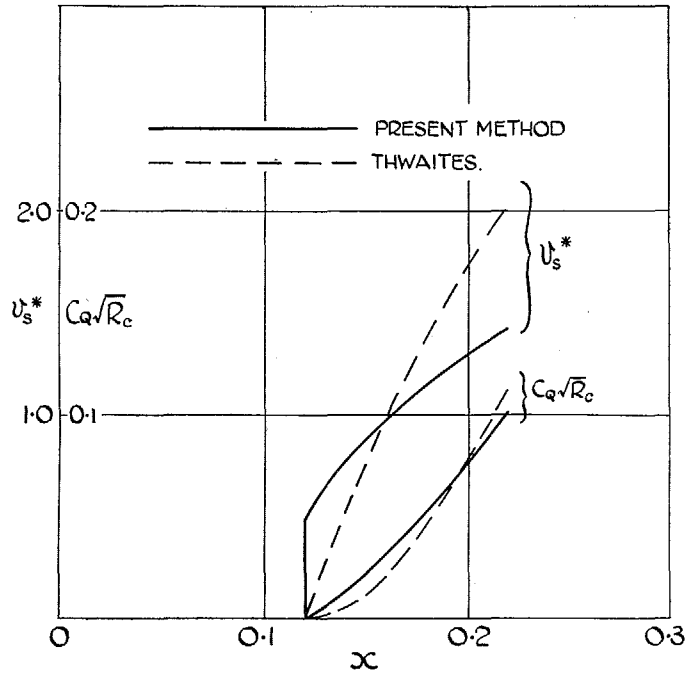


FIG. 10. Comparison of suction distributions given by present calculations and by Thwaites.

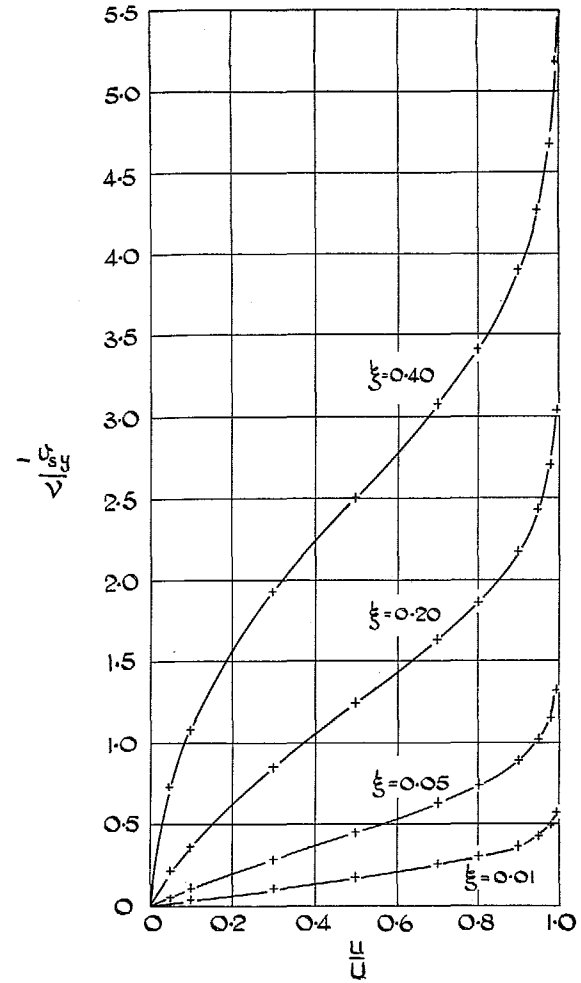


FIG. 11. Velocity profiles for flat plate uniform blowing.

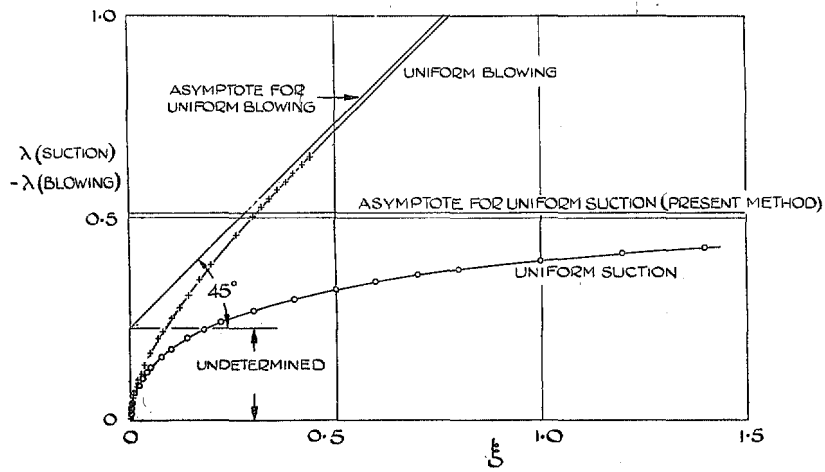


FIG. 12. Comparison of boundary-layer development with uniform suction and uniform blowing.

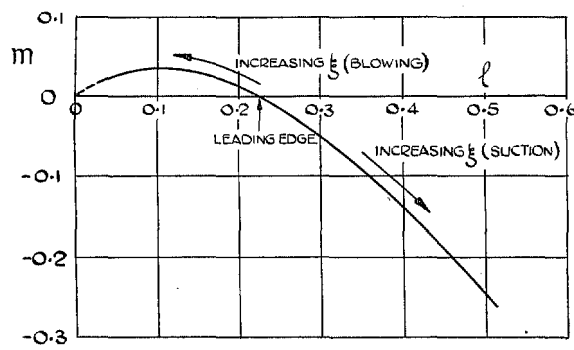


FIG. 13. Comparison of  $l, m$  curves for uniform suction and uniform blowing.

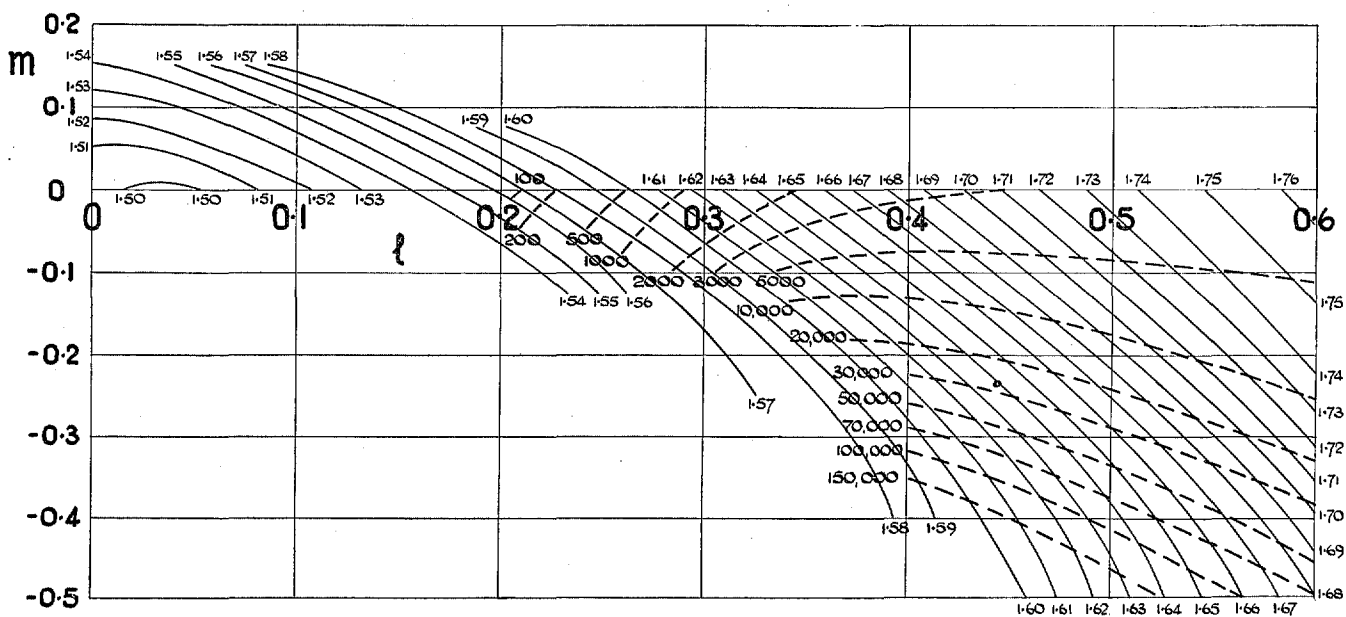


FIG. 14. Chart of  $H_e$  with curves of  $R_{\theta \text{ crit}}$  superimposed.

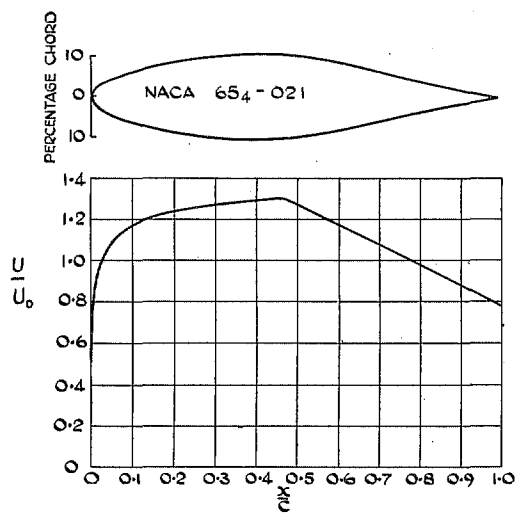


FIG. 15. Basic velocity distribution.

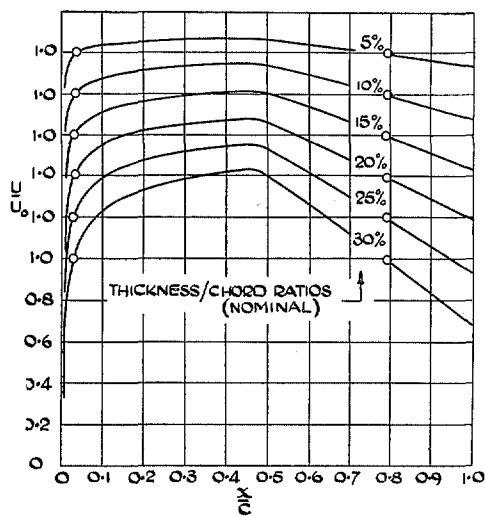


FIG. 16. Velocity distributions used in calculations.

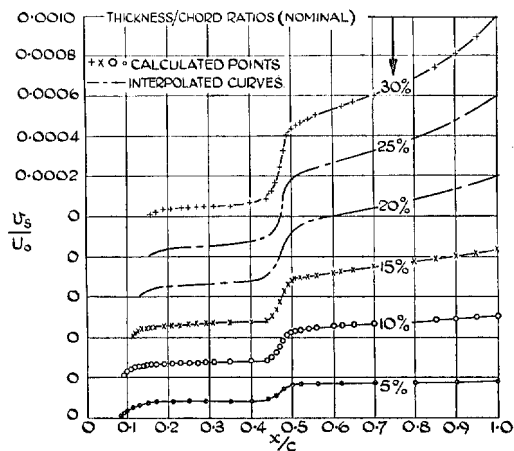


FIG. 17. Distributions of suction velocity for  $R_c = 20 \times 10^6$ .

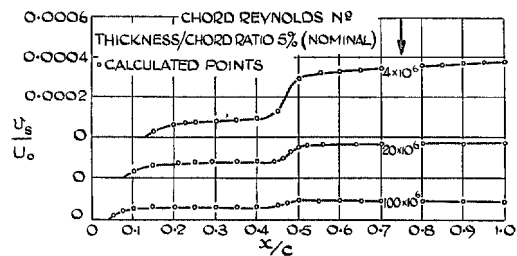
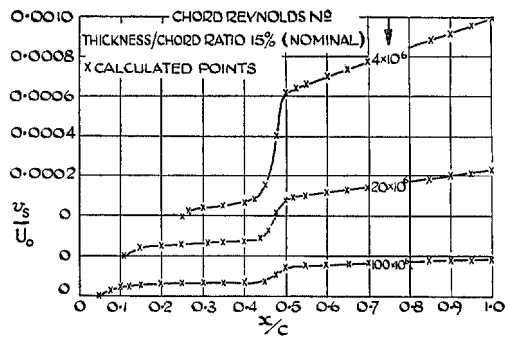


FIG. 18. Distributions of suction velocity for three chord Reynolds numbers.

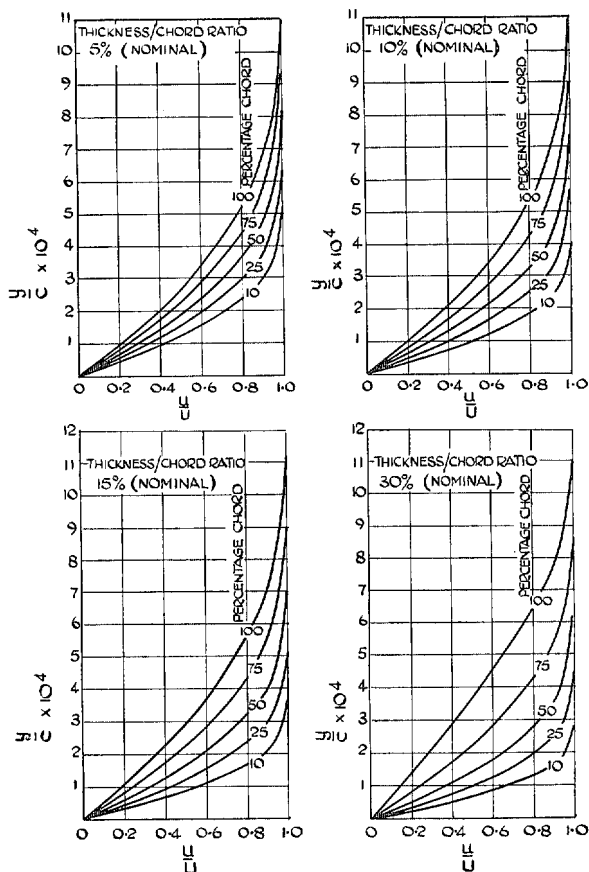


FIG. 19. Velocity profiles for distributions of external velocity and suction velocity shown in Figs. 16 and 17.

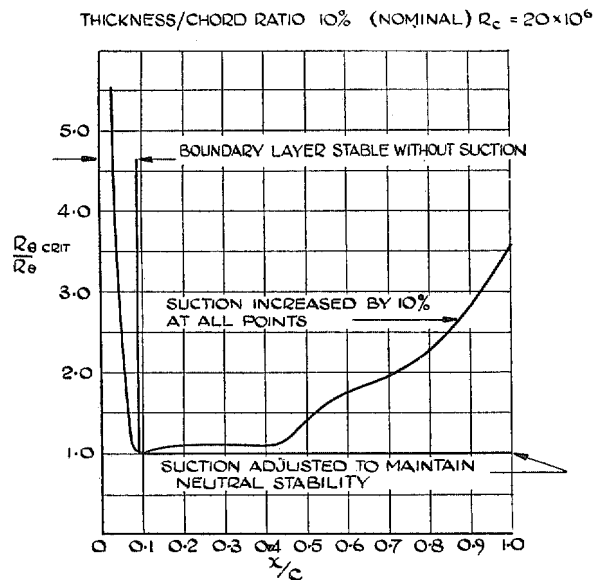


FIG. 20. Effect of small increase in suction velocities on stability of the laminar layer.

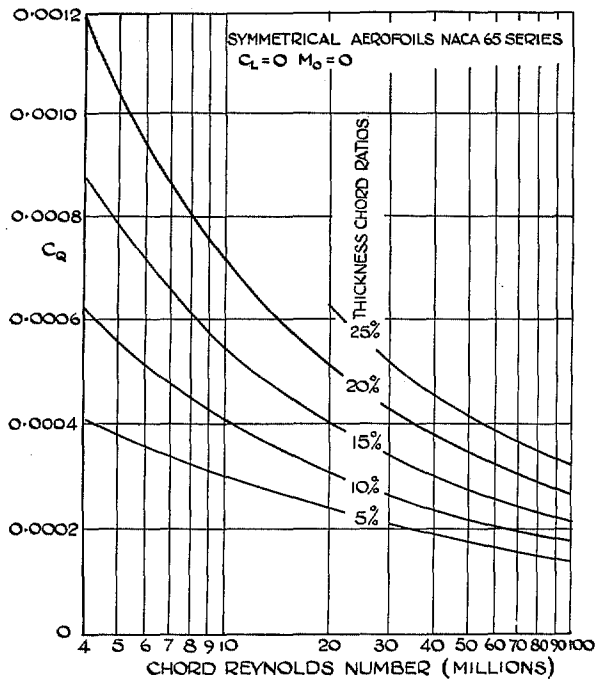


FIG. 21. Variation of suction quantity coefficients with Reynolds number.

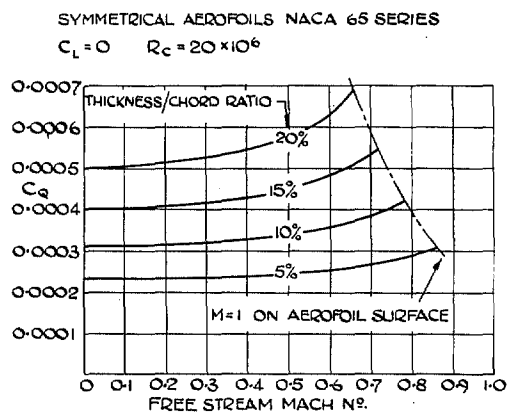
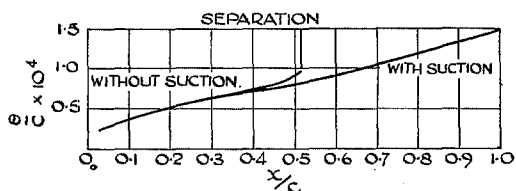
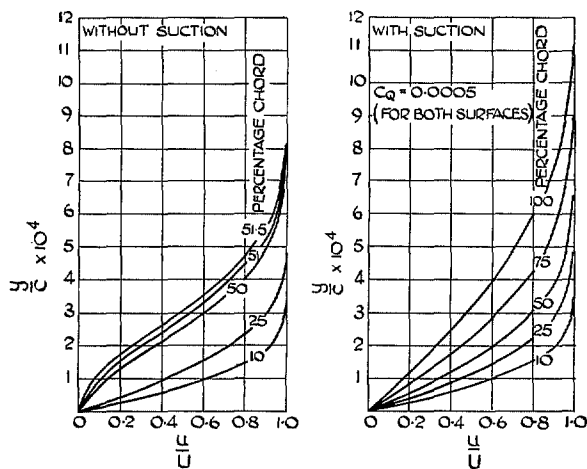


FIG. 22. Variation of suction quantity coefficients with free stream Mach number.

THICKNESS/CHORD RATIO 20% (NOMINAL)  
 CHORD REYNOLDS N<sup>o</sup> = 20 x 10<sup>6</sup>



INCREASE OF MOMENTUM THICKNESS ALONG SURFACE.



VELOCITY PROFILES WITHOUT AND WITH SUCTION

FIG. 23. Development of laminar boundary layer with and without suction.

## Publications of the Aeronautical Research Council

### ANNUAL TECHNICAL REPORTS OF THE AERONAUTICAL RESEARCH COUNCIL (BOUND VOLUMES)

- 1939 Vol. I. Aerodynamics General, Performance, Airscrews, Engines. 50s. (52s.).  
Vol. II. Stability and Control, Flutter and Vibration, Instruments, Structures, Seaplanes, etc. 63s. (65s.)
- 1940 Aero and Hydrodynamics, Aerofoils, Airscrews, Engines, Flutter, Icing, Stability and Control, Structures, and a miscellaneous section. 50s. (52s.)
- 1941 Aero and Hydrodynamics, Aerofoils, Airscrews, Engines, Flutter, Stability and Control, Structures. 63s. (65s.)
- 1942 Vol. I. Aero and Hydrodynamics, Aerofoils, Airscrews, Engines. 75s. (77s.)  
Vol. II. Noise, Parachutes, Stability and Control, Structures, Vibration, Wind Tunnels. 47s. 6d. (49s. 6d.)
- 1943 Vol. I. Aerodynamics, Aerofoils, Airscrews. 80s. (82s.)  
Vol. II. Engines, Flutter, Materials, Parachutes, Performance, Stability and Control, Structures. 90s. (92s. 9d.)
- 1944 Vol. I. Aero and Hydrodynamics, Aerofoils, Aircraft, Airscrews, Controls. 84s. (86s. 6d.)  
Vol. II. Flutter and Vibration, Materials, Miscellaneous, Navigation, Parachutes, Performance, Plates and Panels, Stability, Structures, Test Equipment, Wind Tunnels. 84s. (86s. 6d.)
- 1945 Vol. I. Aero and Hydrodynamics, Aerofoils. 130s. (132s. 9d.)  
Vol. II. Aircraft, Airscrews, Controls. 130s. (132s. 9d.)  
Vol. III. Flutter and Vibration, Instruments, Miscellaneous, Parachutes, Plates and Panels, Propulsion. 130s. (132s. 6d.)  
Vol. IV. Stability, Structures, Wind Tunnels, Wind Tunnel Technique. 130s. (132s. 6d.)

### Annual Reports of the Aeronautical Research Council—

1937 2s. (2s. 2d.)      1938 1s. 6d. (1s. 8d.)      1939-48 3s. (3s. 5d.)

### Index to all Reports and Memoranda published in the Annual Technical Reports, and separately—

April, 1950      -      -      -      R. & M. 2600 2s. 6d. (2s. 10d.)

### Author Index to all Reports and Memoranda of the Aeronautical Research Council—

1909—January, 1954      R. & M. No. 2570 15s. (15s. 8d.)

### Indexes to the Technical Reports of the Aeronautical Research Council—

December 1, 1936—June 30, 1939	R. & M. No. 1850	1s. 3d. (1s. 5d.)
July 1, 1939—June 30, 1945	R. & M. No. 1950	1s. (1s. 2d.)
July 1, 1945—June 30, 1946	R. & M. No. 2050	1s. (1s. 2d.)
July 1, 1946—December 31, 1946	R. & M. No. 2150	1s. 3d. (1s. 5d.)
January 1, 1947—June 30, 1947	R. & M. No. 2250	1s. 3d. (1s. 5d.)

### Published Reports and Memoranda of the Aeronautical Research Council—

Between Nos. 2251-2349	R. & M. No. 2350	1s. 9d. (1s. 11d.)
Between Nos. 2351-2449	R. & M. No. 2450	2s. (2s. 2d.)
Between Nos. 2451-2549	R. & M. No. 2550	2s. 6d. (2s. 10d.)
Between Nos. 2551-2649	R. & M. No. 2650	2s. 6d. (2s. 10d.)
Between Nos. 2651-2749	R. & M. No. 2750	2s. 6d. (2s. 10d.)

*Prices in brackets include postage*

### HER MAJESTY'S STATIONERY OFFICE

York House, Kingsway, London W.C.2; 423 Oxford Street, London W.1; 13a Castle Street, Edinburgh 2;  
39 King Street, Manchester 2; 2 Edmund Street, Birmingham 3; 109 St. Mary Street, Cardiff; Tower Lane, Bristol 1;  
80 Chichester Street, Belfast, or through any bookseller.

S.O. Code No. 23-3124